

Atmospheric studies with the Multi-angle Imaging SpectroRadiometer (MISR)

David J. Diner and the MISR Science Team

Jet Propulsion Laboratory, California Institute of Technology, MS 169-237, 4800 Oak Grove Drive, Pasadena, CA 91109

Telephone (818) 354-6319; Fax (818) 393-4619; E-mail David.J.Diner@jpl.nasa.gov

Abstract: Multi-angle Imaging SpectroRadiometer observations facilitate new atmospheric remote sensing methods. Angular variation of radiometric and geometric scene attributes, in conjunction with new algorithms, enables retrieval of aerosol properties, cloud heights, and cloud-tracked winds.

© 2000 Optical Society of America

OCIS codes: (280.1100) Aerosol detection; (290.1090) Aerosol and cloud effects

1. Introduction

The MISR instrument [1] was launched into polar Earth orbit aboard the Terra spacecraft on December 18, 1999 and the instrument cover was opened on February 24, 2000. Terra is in a 16-day repeat 705-km sun-synchronous orbit, and has approximately a 10:45 am equator crossing time on the descending node. MISR provides multiple-angle, continuous imagery of the Earth in reflected sunlight. It uses nine separate charge coupled device (CCD)-based pushbroom cameras to observe the Earth at nine discrete angles: one at nadir, plus eight other symmetrically placed cameras that provide fore-aft observations with view angles, at the Earth's surface, of 26.1°, 45.6°, 60.0°, and 70.5° relative to the local vertical. Imagery in four spectral bands (blue--446.4 nm, green--557.5 nm, red--671.7 nm, and near-infrared--866.4 nm) is provided at each angle, yielding a total of 36 image channels (9 angles x 4 bands). The spatial sampling is commandable, through flight software, to 275 m, 550 m, or 1.1 km. The nominal global observing mode of the instrument provides 275-m sampling in all bands of the nadir camera and the red band of each of the off-nadir cameras, and 1.1 km for the remaining 24 channels. It takes 7 minutes to observe any given scene at all 9 angles. The images are linearly quantized to 14 bits, then square-root compressed to 12 bits before transmission. MISR operates continuously on the day side of every Terra orbit.

MISR's cameras have progressively increasing focal lengths as the view angle increases in order to preserve cross-track resolution as a function of angle. A nomenclature has been devised to provide a shorthand way of referring to the individual cameras. The designation An is used for the nadir view; the forward-viewing four cameras are designated Af, Bf, Cf, and Df in order of increasing off-nadir angle; and the aftward-viewing bank is designated Aa, Ba, Ca, and Da. Here, A, B, C, D refer to the effective focal lengths of the camera lenses (approximately 59, 73, 95, and 124 mm, respectively). The A design is used for the nadir as well as near-nadir cameras, providing slightly higher resolution in the raw nadir camera imagery; however, the resampled and georectified data are placed on equal scale grids. On-board calibration hardware provides high radiometric accuracy and stability of the data. This observing strategy enables the use of radiative transfer theory and physically-based models to facilitate the retrieval of aerosol and cloud properties.

2. Data Processing

Raw MISR data undergo a series of processing steps in order to produce radiance imagery in preparation for geophysical retrievals. First, the data are radiometrically scaled using a set of calibration coefficients for each detector [2]. Then, using a geometrically calibrated camera model, image spatial co-registration is accomplished [3]. A common grid for the georectified radiances is established to provide the required co-registration. Space-Oblique Mercator (SOM) is used for this grid because its projection meridian nominally follows the spacecraft ground track and a constant distance scale is preserved along that track, thus minimizing distortion and resampling effects. The map resolution of the projection is matched to the horizontal sampling mode of each camera channel.

A separate projection is established for each of the paths of the 233 repeat orbits of the EOS 16-day cycle. Two types of SOM projection are used for MISR data: terrain projection, in which the images are mapped to a surface defined by a digital elevation model (DEM) in order to account for angle-dependent topographically induced misregistrations; and ellipsoid projection, in which the images are mapped to a surface defined by the WGS84 ellipsoid. The former is used for aerosol retrievals, since the retrieval algorithms require the surface-leaving radiances to correspond to the same point on the surface terrain. Stereoscopic cloud height and wind retrievals make use of the ellipsoid-projected data.

3. Geophysical Retrievals

The retrieval of aerosol optical depth over land from space is a difficult challenge owing to the brightness and heterogeneity of the land surface. However, multi-angle imagery provides the opportunity to use the enhanced slant paths and variation in signal with angle to detect and characterize atmospheric hazes. One example of this capability is a set of images shown in Figure 1, obtained on March 6, 2000 over the eastern United States and encompassing Lake Ontario to Georgia. The left image is a nadir view, and the middle image is from camera Df. At the larger slant angle, the line-of-sight through the atmosphere is longer and a haze over the Appalachian Mountains is significantly more apparent. The right-hand image shows retrieved 558-nm optical depth. Over land, the retrieval utilizes spatial contrasts in the imagery and establishes a representation of the angular shape of the surface component of the reflectance using empirical orthogonal functions [4]. The aerosol optical depth is then derived from fitting the angular shape of the remaining signal to modeled atmospheric path radiances. Over water, a prescribed surface model is used in combination with models of atmospheric path radiance. Aerosol retrievals are performed on $17.6 \times 17.6 \text{ km}^2$ regions, and thus at coarser resolution than the underlying imagery. Despite the use of completely different algorithms over land and water, the retrieved optical depth is roughly continuous across the land/water boundary at the lower right. Retrieved 558-nm optical depth in the hazier areas is ~ 0.2 .

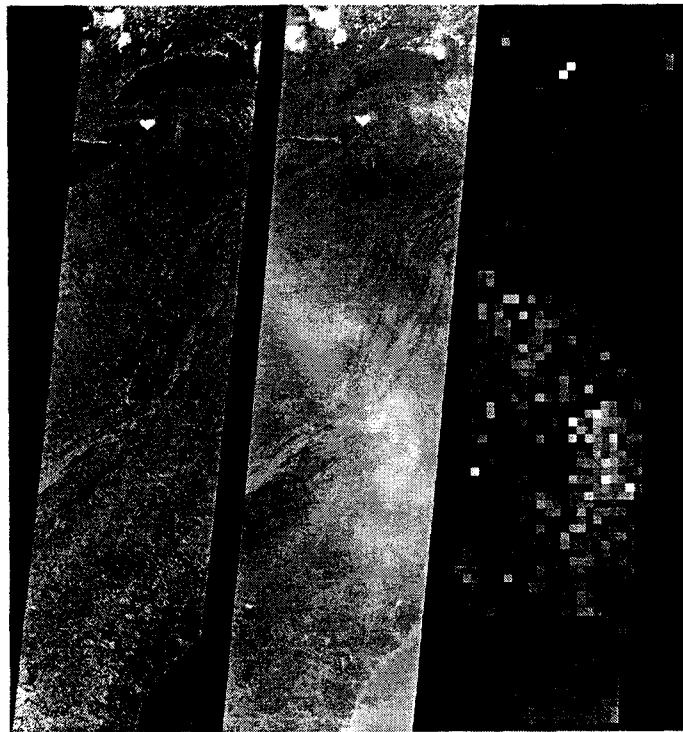


Figure 1. The eastern US, March 6, 2000. Left: Nadir top-of-atmosphere (TOA) image. Middle: Df TOA image. Right: Retrieved 558-nm aerosol optical depth field. North is at the top.

In studies of cloud-climate interactions, accurate cloud height is one of the principal characteristics required to model the three-dimensional field of radiative fluxes. In order to establish a classification scheme incorporating cloud altitudes, a reference level known as the Reflecting Level Reference Altitude is defined. The RLRA is the level found by matching features (or areas) with the greatest contrast in the near-nadir viewing directions. This corresponds to the main reflecting layer, which will typically be either the tops of clouds, or under clearer conditions, the surface. The RLRA is defined over areas measuring $2.2 \times 2.2 \text{ km}^2$.

The algorithm for retrieving RLRA is stereophotogrammetric, and uses a combination of area and feature matching algorithms to measure the displacement between clouds from one MISR view to another. This displacement results from geometric parallax due to the cloud's height above the surface ellipsoid, plus actual motion driven by wind. Multiple views obtained from satellite altitude over a wide angular range provide the ability to separate the effects of wind displacement from height [5]. Winds are retrieved over mesoscale domains measuring $70.4 \times 70.4 \text{ km}^2$. An

example retrieval is shown in Figure 2, derived from data acquired on August 21, 2000. The left image is a nadir view, and shows the eastern edge of Hurricane Debby in the mid-Atlantic. To the right of this image is the derived RLRA field. Brighter areas correspond to higher clouds. The rightmost image superimposes the retrieved wind vectors. The longest vector corresponds to the highest wind speed of ~ 30 m/sec.

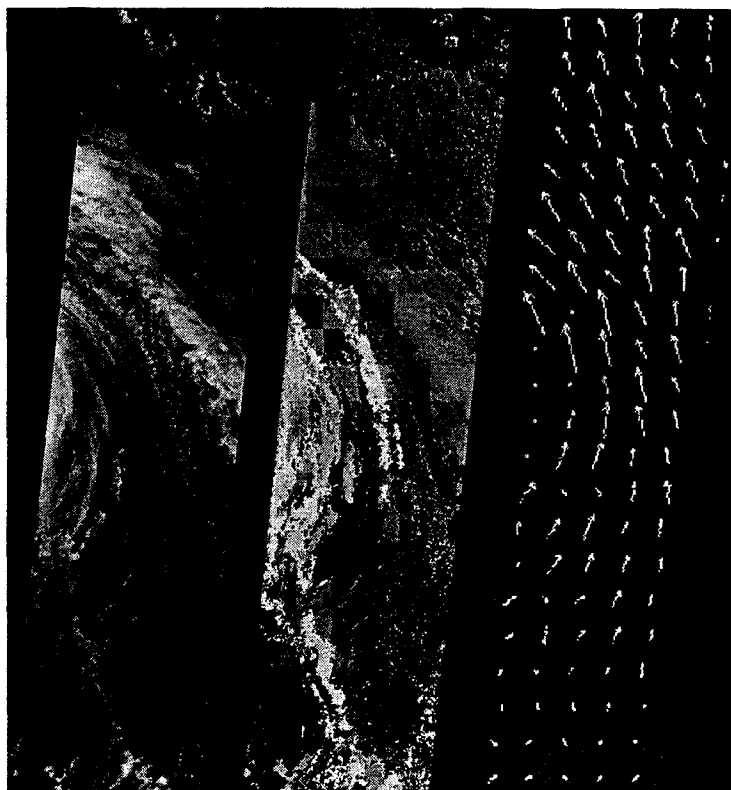


Figure 2. Eastern edge of Hurricane Debby, August 21, 2000. Left: Nadir image. Middle: Retrieved RLRA field. Right: Retrieved cloud-tracked wind vectors. North is at the top.

4. Conclusions

New algorithms have been developed to capitalize on the unique nature of MISR data. These first-generation algorithms will likely be refined as a result of more experience and validation efforts. Data are processed and archived at the NASA Langley Atmospheric Sciences Data Center (<http://eosweb.larc.nasa.gov>). Overall, MISR is performing superbly (see <http://www-misr.jpl.nasa.gov> for more information about the experiment and mission). This work is being carried out at the Jet Propulsion Laboratory, California Institute of Technology, under contract with the National Aeronautics and Space Administration.

5. References

1. D. Diner, J. Beckert, T. Reilly, C. Bruegge, J. Conel, R. Kahn, J. Martonchik, T. Ackerman, R. Davies, S. Gerstl, H. Gordon, J-P. Muller, R. Myneni, P. Sellers, B. Pinty, and M. Verstraete, "Multi-angle Imaging SpectroRadiometer (MISR) instrument description and experiment overview," *IEEE Trans. Geosci. Rem. Sens.* **36**, pp. 1072-1087 (1998).
2. C.J. Bruegge, D.J. Diner, and V.G. Duval, "The MISR calibration program," *J. Atmos. Ocean. Tech.* **13**, pp. 286-299 (1996).
3. V.M. Jovanovic, M.M. Smyth, J. Zong, R. Ando, and G.W. Bothwell, "MISR photogrammetric data reduction for geophysical retrievals," *IEEE Trans. Geosci. Rem. Sens.* **36**, pp. 1290-1301 (1998).
4. J.V. Martonchik, D.J. Diner, R.A. Kahn, T.P. Ackerman, M.M. Verstraete, B. Pinty, and H.R. Gordon, "Techniques for the retrieval of aerosol properties over land and ocean using multiangle imaging," *IEEE Trans. Geosci. Rem. Sens.* **36**, pp. 1212-1227 (1998).
5. D.J. Diner, R. Davies, L. Di Girolamo, A. Horvath, C. Moroney, J-P. Muller, S.R. Paradise, D. Wenkert, and J. Zong, "MISR Level 2 Cloud Detection and Classification Algorithm Theoretical Basis," JPL Document D-11399, Rev. D (1999). Available at <http://eospsa.gsfc.nasa.gov/atbd/misrtables.html>.